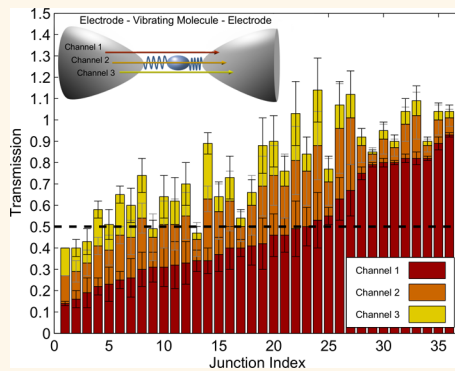


Electron–Vibration Interaction in Multichannel Single-Molecule Junctions

Regev Ben-Zvi, Ran Vardimon, Tamar Yelin, and Oren Tal*

Department of Chemical Physics, Weizmann Institute of Science, Rehovot, 76100 Israel

ABSTRACT The effect of electron–vibration interaction in atomic-scale junctions with a single conduction channel was widely investigated both theoretically and experimentally. However, the more general case of junctions with several conduction channels has received very little attention. Here we study electron–vibration interaction in multichannel molecular junctions, formed by introduction of either benzene or carbon dioxide between platinum electrodes. By combining shot noise and differential conductance measurements, we analyze the effect of vibration activation on conductance in view of the distribution of conduction channels. Based on the shift of vibration energy while the junction is stretched, we identify vibration modes with transverse and longitudinal symmetry. The detection of different vibration modes is ascribed to efficient vibration coupling to different conduction channels according to symmetry considerations. While most of our observations can be explained in view of the theoretical models for a single conduction channel, the appearance of conductance enhancement, induced by electron–vibration interaction, at high conductance values indicates either unexpected high electron–vibration coupling or interchannel scattering.



KEYWORDS: molecular junction · electron–vibration interaction · conduction channel · molecular electronics · vibration mode · electronic transport

In the attempt to control and manipulate conductance at the atomic scale, great focus has been given to single-atom and single-molecule junctions, due to their simplicity in the first case and their structural versatility in the second. According to the Landauer picture, electrons are transmitted across these junctions through a limited number of conduction channels resulting from the electronic quantization at the junction constriction.^{1,2} The conduction channels are the eigenstates of the scattering matrix that relates incoming and outgoing electronic modes in the junction constriction. Each channel can carry a conductance of up to $1G_0$ ($G_0 = 2e^2/h$ is the quantum of conductance). Revealing the distribution of conduction channels has great importance for understanding different aspects of atomic-scale conductance.^{3–5} One of the most fascinating aspects of such junctions is the effect of vibrations on electronic transport properties of these atomic-scale electromechanical systems. Interestingly, far from electronic resonance, the activation

of electron–vibration interactions can either enhance or suppress the conductance.^{6–9} This phenomenon was widely studied both experimentally and theoretically in the context of atomic-scale junctions with a single conduction channel.^{7,8,10–26} However, in the general case of junctions with several conduction channels, the effect of electron–vibration interaction was never studied in view of different channel distributions.

When the applied voltage across a molecular or atomic junction is equal to or higher than the energy of a certain vibration mode ($eV \geq \hbar\omega$), the mode can be excited by interaction with the conduction electrons. For weak electron–vibration coupling in the off-resonance regime, the onset of vibration activation gives rise to a small inelastic current, which is manifested as a step in the measured differential conductance^{27,28} (e.g., Figure 1a,b). This interpretation was verified by vibration energy shifts induced by isotopic substitution.^{6,8,29} The influence of vibration activation on the conductance of molecular junctions is widely used as a

* Address correspondence to oren.tal@weizmann.ac.il.

Received for review September 17, 2013 and accepted November 19, 2013.

Published online November 19, 2013
10.1021/nn404873x

© 2013 American Chemical Society

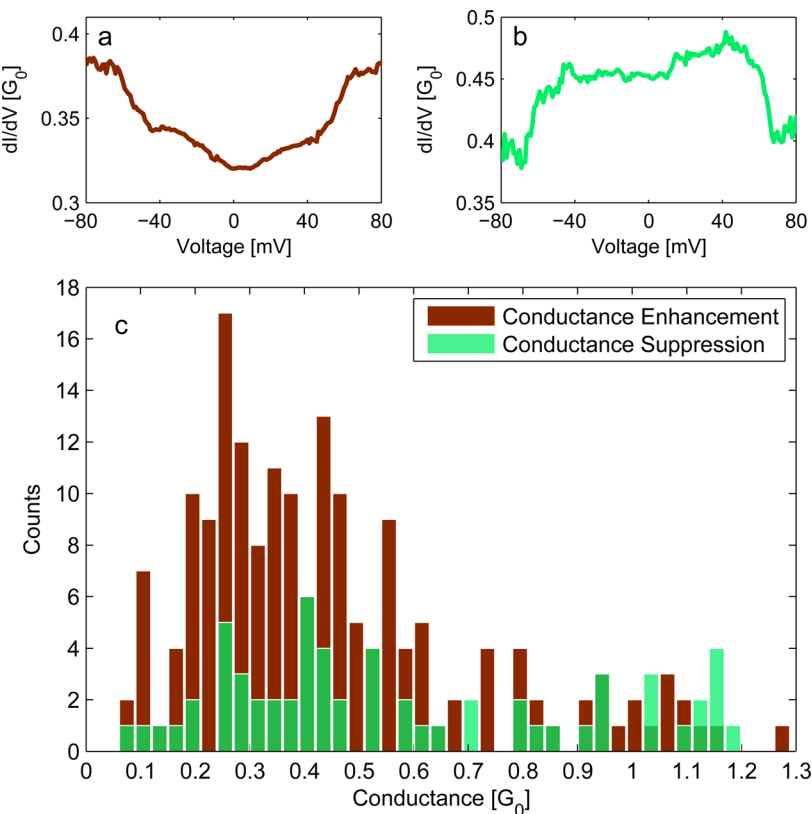


Figure 1. (a, b) Step-like feature in the differential conductance (dI/dV) spectrum as a function of bias voltage, observed for two different Pt/benzene molecular junctions. The onset of vibration is manifested as conductance enhancement in (a) and conductance suppression in (b). (c) Histogram of conductance enhancement (red) and suppression (green), observed in dI/dV spectra, as a function of zero-bias conductance for Pt/benzene molecular junctions. Note that overlapping counts appear as dark green.

characterization tool in the study of charge transport at the atomic scale. It allows the detection and chemical recognition of a molecule in the junction and provides information on the close relation between structure and conductance.^{9,29–36}

When the incoming electrons activate a vibration mode, the conductance can be either enhanced or suppressed. The opposite response was observed in two different conductance limits. Conductance enhancement is typically found at conductance values much lower than $1G_0$.⁶ In the other limit, of conductance close to $1G_0$, suppression of conductance is typically found for junctions that are characterized by a fully open single conduction channel.^{7,29} Since in many cases differential conductance is measured in systems with conductance at one of these two limits, the effect of vibration activation in the intermediate range of conductance is not readily accessible.

A single molecule connected directly to the electrodes (*i.e.*, with no anchoring groups such as thiols) is an attractive candidate for the study of electron–vibration interaction. By changing the interelectrode displacement in a break junction setup,³⁷ a wide range of conductance values can be probed^{38,39} and the effect of vibration activation can be investigated in different conductance regimes. In the case of directly

linked molecules, the bias-voltage window of the measurement is limited by the junction stability at high current densities. When considering the possible vibration modes of such a molecular junction, one should distinguish between the internal vibration modes of the molecule and vibration modes that correspond to the motion of the entire molecule with respect to the electrodes. Due to their lower excitation energy, the latter modes are more likely to appear in the bias window accessible in these measurements.^{8,34,38} These vibration modes can be classified as longitudinal or transverse modes, describing motion along or perpendicular to the junction axis, respectively. The symmetry of the vibration modes can be determined from the evolution of vibration energy as a function of applied tension when increasing the interelectrode displacement. Longitudinal modes are characterized by a decrease in the vibration energy when stretching the junction. This response results from weakening of bonds between the molecule and the electrodes. Transverse modes, however, are characterized (at a certain stretching range) by an increase in the vibration energy due to a larger restoring force.⁸ The classification as longitudinal or transverse modes can be useful since the coupling between vibration modes and conduction channels is determined by their symmetry.

According to several calculations in the limit of weak electron–vibration coupling that take into consideration a single elastic conduction channel as a starting point, the effect of vibration activation on conductance depends on the transmission probability of electrons crossing the junction and the symmetry of the molecule–electrode coupling.^{10,11,16,17,19–25,40} Many of these single-channel models are based on the nonequilibrium Green function formalism and present a competition between elastic and inelastic processes.¹¹ For symmetric molecule–electrode coupling, the first process suppresses the conductance and it is the dominant effect at a transmission probability $\tau > 0.5$, while the second one enhances the conductance and it is dominant at $\tau < 0.5$ (*i.e.*, a crossover at $\tau = 0.5$).^{10,11} For an asymmetric coupling to the electrodes, the transmission probability at the crossover is expected to be lower than 0.5, and it is decreased as the asymmetry of the coupling to the electrodes increases.^{23,40} It is worth mentioning that the predicted crossover is not universal,^{20,22} and it is valid only when the vibration energy is much smaller than the coupling energy between the molecule and the electrodes and from the Fermi energy vs the relevant molecular level difference. Practically, the crossover was experimentally observed for several molecular junctions,^{13,38,41} indicating that these conditions are valid in these cases.

Recently, Nakazumi *et al.* used a single-channel model to explain the observation of a crossover between conductance enhancement and suppression by vibration activation for a certain molecular junction and the lack of a crossover for a different junction. According to the authors, the crossover is not apparent when there are several conduction channels, and the model cannot be applied in such a case.⁴¹ On the contrary, a clear crossover was observed in the case of Pt/H₂O junctions for which more than a single channel was found experimentally.³⁸ Clearly, the influence of vibrations on the electronic transport across atomic-scale junctions is far from being well understood in the general case of junctions with more than a single conduction channel.

In this paper we focus on molecular junctions with several conduction channels: Pt/benzene and Pt/CO₂. The conditions that lead to conductance enhancement and suppression are studied. For Pt/benzene junctions, both conductance enhancement and suppression are detected throughout the entire range of conductance values. On the other hand, for Pt/CO₂ junctions, conductance enhancement is observed mainly below a conductance value of 0.7G₀ and conductance suppression is observed mainly above a conductance value of 0.8G₀. These findings are addressed in the framework of multichannel junctions by differential conductance and shot noise measurements. Using the models for a single channel as our starting point, the role of channel

distribution as well as the experimentally observed symmetry of different vibration modes is considered.

RESULTS AND DISCUSSION

The conditions for conductance enhancement and suppression, induced by the onset of vibrations, are studied by differential conductance (d/dV) measurements, taken on random molecular junction configurations with different conductance values. The junctions were formed using the mechanically controllable break junction technique.³⁷ Following the formation of molecular junction,³⁴ the contact is squeezed up to a large conductance value of $\sim 70G_0$. Then the electrodes are pulled apart until a stable contact is formed at a conductance value lower than 1.5G₀, which is the typical conductance of a single Pt atom.²⁹ At this point the interelectrode spacing is fixed and a d/dV spectrum is recorded while the dc voltage between the electrodes is swept (for more details see the Methods section).

Figure 1a,b show two examples for d/dV spectra, measured as a function of voltage across two independent Pt/benzene junctions. The onset of vibrations, indicated by a step-like change in the conductance, is observed. While in (a) the activation of vibrations is manifested as conductance enhancement, in (b) it appears as conductance suppression. The distribution of spectra with conductance enhancement (red) and conductance suppression (green) is presented in Figure 1c as a function of zero-voltage conductance. The histogram presents measurements taken on 300 independent Pt/benzene junctions.

For the Pt/benzene junctions, both conductance enhancement and suppression are observed in the entire range of conductance values, as opposed to the simple models for symmetric junctions with a single conduction channel, where conductance enhancement and suppression are predicted below and above 0.5G₀, respectively. In order to understand this behavior, the number of conduction channels, their transmission probabilities τ , and possible molecule–electrode asymmetric coupling need to be considered. Paulsson *et al.* showed that in a model that considers a single transmission channel and asymmetric molecule–electrode coupling, the crossover between conductance enhancement and suppression can take place at conductance values lower than 0.5G₀.⁴⁰ Such asymmetry is expected for Pt/benzene junctions since Pt monatomic chains can be pulled from the electrodes to form hybrid structures, in which the molecule is preferentially bonded to one electrode on one side and connected to a Pt atomic chain on the other side.³⁹

The occurrence of conductance enhancement at relatively high conductance values can be explained in view of the distribution of conduction channels at the junction. Theoretical and experimental studies of transmission probabilities in Pt/benzene junctions^{33,42} reveal up to three conduction channels. The number of

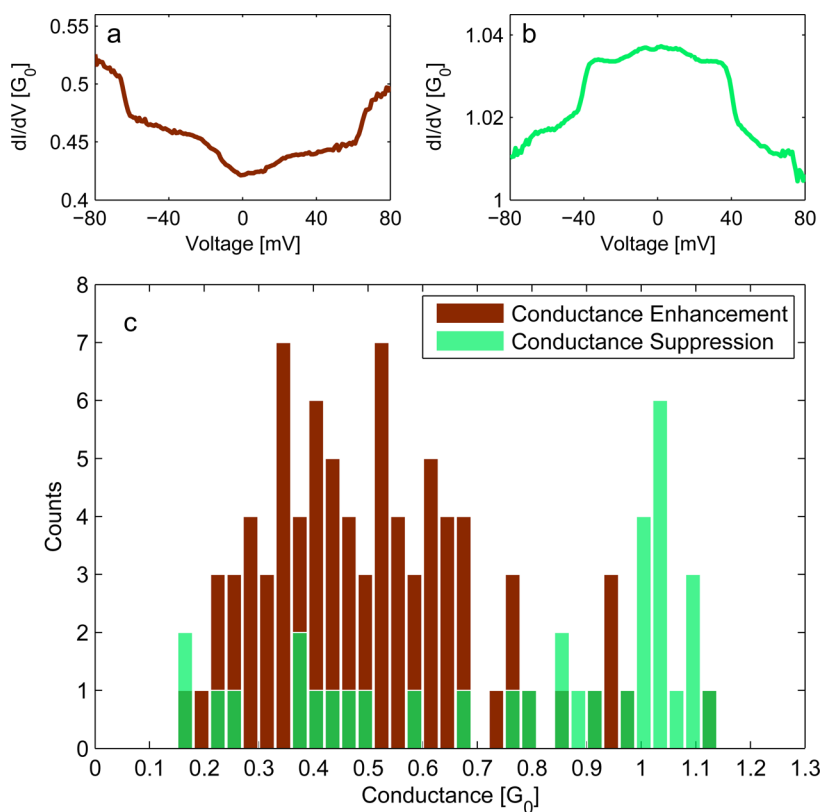


Figure 2. (a, b) Step-like feature in the differential conductance (dI/dV) spectrum as a function of bias voltage, observed for two different Pt/CO₂ molecular junctions. The onset of vibration is manifested as conductance enhancement in (a) and conductance suppression in (b). (c) Histogram of conductance enhancement (red) and suppression (green), observed in dI/dV spectra, as a function of zero-bias conductance for Pt/CO₂ molecular junctions. Note that overlapping counts appear as dark green.

conduction channels as well as their transmission is determined by the specific orientation of the molecule with respect to the electrode apexes. The total conductance is given by the sum of contributions from each channel, $G = G_0 \sum \tau_n$, where τ_n is the transmission probability of the n th channel.^{1,2} Both the calculated transmission probabilities and the probabilities found experimentally by shot noise measurements indicate the presence of several partly transmitting channels with comparable transmissions. For Pt/benzene junctions with conductance above $0.5G_0$, the total conductance is composed of two or three channels, which often have transmission probabilities smaller than 0.5. Thus, the appearance of conductance enhancement at large conductance values is expected. The propensity of benzene to form asymmetric hybrid junctions with Pt electrodes³⁹ and the lack of a dominant conduction channel coupled to a vibration mode³³ can explain the detection of conductance enhancement and suppression throughout the entire conductance range. In this case the results can be explained by considering the single-channel models for each channel independently.

The response of conductance to vibration activation in the case of Pt/CO₂ junctions reveals a different picture (Figure 2). Although there is no sharp value for

the crossover between curves with conductance enhancement and suppression, the former appears mostly below $0.7G_0$, and the latter appears mainly above $0.8G_0$. Interestingly, the observed crossover takes place at a conductance value higher than the expected value of $0.5G_0$, for a symmetric junction with a single channel. Unlike for Pt/benzene junctions, we do not have former theoretical or experimental information about the channel distribution, which is essential for understanding the interplay between electronic transport and vibration modes in these junctions. Therefore, we performed shot noise measurements on Pt/CO₂ molecular junctions at different conductance values.

Electronic shot noise in atomic-scale junctions originates from current fluctuations due to the discrete nature of the flow of electrons. This noise depends on the number of transmission channels, N , as well as their transmission probabilities, τ_n .⁴³ For $eV \gg kT$, shot noise is given by $S = 2eI/F$, where e is the electron charge, I is the current, and $F = \sum_{n=1}^N \tau_n (1 - \tau_n) / \sum_{n=1}^N \tau_n$ is the Fano factor. The Fano factor can be extracted from the dependence of noise on the applied bias current and provides an independent equation (apart from $G = G_0 \sum_{n=1}^N \tau_n$) that depends on the transmission probabilities. Thus, shot noise and conductance measurements

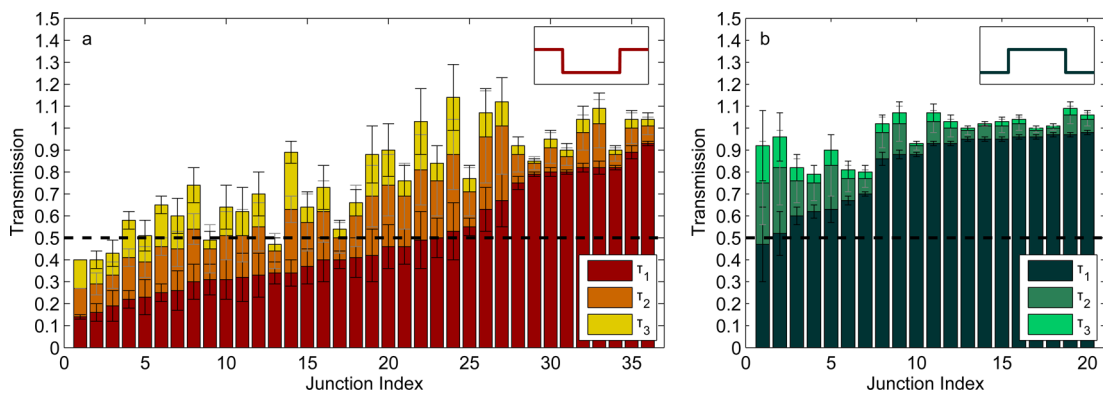


Figure 3. Channel distribution obtained from shot noise measurements for Pt/CO₂ molecular junctions. (a) Channel distribution of junctions that showed conductance enhancement in their dI/dV spectrum and (b) conductance suppression, due to vibration activation. The error bars represent the range of solutions that satisfies the measured conductance and shot noise.⁴⁴

can be used to analytically find the transmission probabilities for the case of at most two channels. However, we cannot determine *a priori* that the number of conduction channels in Pt/CO₂ junctions is restricted to two. We overcome this limitation by relaxing the requirement for exact determination of the transmission probabilities. The transmission probabilities of each conduction channel is then determined with a limited accuracy.⁴⁴ Here, shot noise measurements were performed along with dI/dV measurements in order to study the relation between channel distribution and the effect of electron–vibration interaction.

Figure 3 presents the transmission probabilities of the three main channels extracted from shot noise measurements for different conductance values of Pt/CO₂. The shot noise results are divided according to junctions that showed vibration-induced conductance enhancement (Figure 3a) and suppression (Figure 3b) in the dI/dV spectrum. We note that the appearance of conductance enhancement or suppression was found to be correlated with the classification of the vibration modes as transverse or longitudinal modes, as will be shown. Each column represents the channel distribution measured for a single independent junction. The error bars represent the range of transmission values that satisfy the measured conductance and shot noise.⁴⁴

For all junctions that yield conductance suppression due to vibration activation (Figure 3b), one dominant channel is clearly observed. This dominant channel has a transmission probability (τ_1) larger than 0.5 in the vast majority of measurements (in two measurements the range of solutions does not allow determining whether τ_1 is higher or lower than 0.5). These observations can be explained by applying the single-channel models to the dominant channel.³⁸ Accordingly, the active vibration mode is then coupled to the dominant conduction channel, and its activation is manifested as conductance suppression due to transmission probability larger than 0.5.

Focusing on junctions that showed conductance enhancement (Figure 3a), we can distinguish between

two cases. For junctions 1–23 the conduction channels are more equally distributed and no clear dominant channel exists. In these cases all the channels have transmission probabilities smaller than 0.5. Therefore, vibration activation is expected to yield conductance enhancement, regardless of the channel to which it is coupled. For junctions 24–36 the dominant channel has a transmission probability larger than 0.5. If we apply the basic concepts of the single-channel models to this multichannel case, we can conclude that, in order to have conductance enhancement by vibration activation, the vibration is coupled to one of the secondary conduction channels that have a transmission probability smaller than 0.5. This observation resembles the case of an aluminum point contact,⁴⁵ where different vibration modes couple to different conduction channels, according to symmetry considerations.^{40,46,47}

In order to investigate whether conductance enhancement and suppression in Pt/CO₂ junctions with $\tau_1 > 0.5$ can be a result of the excitation of different vibration modes, we study the symmetry of these modes by their response to strain. This is done by following the vibration energy as the interelectrode distance is increased.^{8,45} Figure 4a presents a sequence of dI/dV spectra, showing conductance enhancement at the onset of vibration activation. Before the next spectrum was recorded the junction was stretched by ~ 0.05 Å. Figure 4b shows the d²I/dV², obtained by numerical derivation of the dI/dV spectrum, from which the energy of the vibration mode (equivalent to the peak voltage in eV) was extracted and is presented as a function of interelectrode separation in Figure 4c. The contact was stretched to an overall distance of about 0.6 Å. Figure 4c shows that the energy of the examined vibration mode is shifted to higher values as the contact is stretched. An increase in the vibration energy, while the junction is stretched, is typical of transverse modes, *i.e.*, a motion of the molecule perpendicular to the junction axis.⁸ A different sequence of dI/dV spectra (Figure 4d) and the associated d²I/dV²

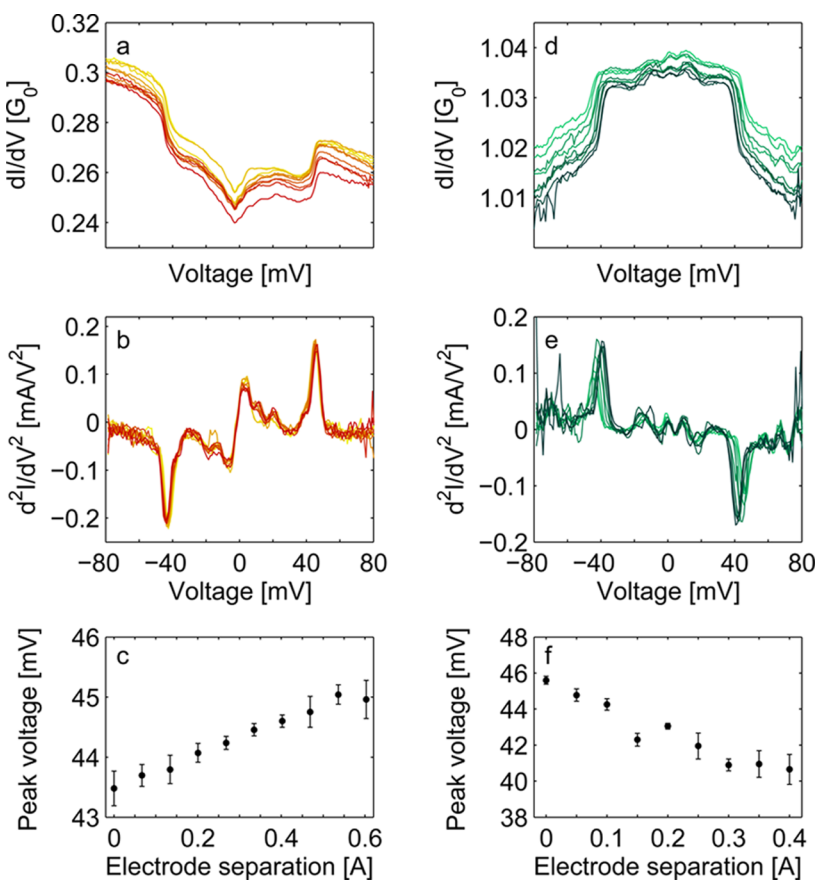


Figure 4. (a) Sequential dI/dV spectra and (b) their numerical derivative (d^2I/dV^2), showing vibration activation manifested as conductance enhancement. The contact was stretched by increasing the interelectrode separation to an overall distance of 0.6 Å between the first (yellow) and the last (red) curve. (c) Vibration voltage (or energy in eV) as a function of electrode separation. (d) Different sequential dI/dV spectra and (e) their numerical derivative (d^2I/dV^2), showing vibration activation manifested as conductance suppression. The contact was stretched to an overall distance of 0.4 Å between the first (light green) and the last (dark green) curve. (f) Vibration voltage as a function of electrode separation.

(Figure 4e) show that the activation of vibration is manifested as conductance suppression. When the junction is stretched, the energy of the vibration mode shifts to lower values (Figure 4f). Based on the observed shift of vibration energy, we conclude that this vibration mode has a longitudinal symmetry with respect to the junction axis. Note that despite the similar energy, the two modes can be clearly distinguished by their opposite response to strain.

A direct correlation is found between the symmetry of the vibration mode and the sign of the conductance change induced by the vibration activation. We recorded five sequences with conductance enhancement, in which the vibration mode was recognized as transverse, and six sequences that show conductance suppression, for which the relevant mode was identified as longitudinal. While dI/dV sequences with conductance suppression and longitudinal symmetry are always found at conductance values of around $1G_0$, dI/dV sequences with conductance enhancement and transverse symmetry were found in a wide conductance range, both below and above $0.5G_0$, corresponding to the distribution of conductance

enhancement and suppression shown in Figures 2 and 3. The conductance suppression resulting from the activation of the longitudinal mode can be understood in the framework of the single-channel model by the coupling of the mode to the dominant channel. The excitation of a transverse mode, on the other hand, was manifested as conductance enhancement, indicating that the vibration is coupled to a secondary channel. However, this scenario leads to an unexpected high electron–vibration coupling. While in similar molecular junctions the change in conductance at the onset of vibration is on the order of a few percent,^{8,34,38} we find here for the relevant junctions (index 24–36 in Figure 3a) a step height of 2–36% with respect to the conductance of the secondary channel. Such a large inelastic contribution to the conductance is interpreted in the context of single-channel models as an indication for a significant electron–vibration coupling. Although we cannot exclude high electron–vibration coupling in Pt/CO₂ junctions, it is unlikely in view of the low coupling found for the junctions mentioned above. Alternatively, the step height in the examined case does not necessarily imply

a strong electron–vibration coupling and multichannel effects should be considered.

In multichannel junctions, electron–vibration interactions can lead to coupling between channels. The probability of such a process depends strongly on the symmetry of the relevant channels and the vibration mode. Using first-principles calculations and scattering theory, Kristensen *et al.* found that vibration activation can lead to conductance enhancement in a Pt/H₂ junction, although this system is characterized by a single almost fully open channel.⁴⁸ According to the authors, transverse vibration modes can couple between a transmitting s-channel and an otherwise nontransmitting d-channel. On the other hand, the symmetry of the longitudinal modes does not allow such coupling, and therefore the excitation of these modes results in conductance suppression in accordance with the models for a single channel. In view of these theoretical findings, the observed conductance enhancement for Pt/CO₂ junctions, when $\tau_1 > 0.5$ (junctions 24–36 in Figure 3a), can result from induced scattering by the transverse vibration mode between the dominant channel and a secondary channel, if these channels have different symmetry. In this scenario the step height should be considered with respect to the dominant channel and the change in conductance is only a few percent, as expected.

CONCLUSIONS

We studied electron–vibration interaction in Pt/benzene and Pt/CO₂ molecular junctions, for which the conductance is carried through several conduction channels. By combining shot noise and differential conductance (dI/dV) measurements, we find the relations between the distribution of conduction channels, the sign of conductance change, and the vibration mode symmetry. For Pt/benzene junctions the models for a single channel can be applied to each channel individually. The appearance of conductance suppression at conductance values lower than 0.5G₀ is explained by the benzene tendency to form asymmetric junctions with asymmetric molecule–electrode coupling. The observed vibration-induced conductance enhancement at conductance higher than 0.5G₀ is

explained by the absence of a dominant channel; that is, the high conductance value, in some stable configurations, is composed of two or more conduction channels with $\tau < 0.5$.

For Pt/CO₂ junctions, vibration-induced conductance suppression is observed mainly above 0.8G₀. In agreement, shot noise measurements reveal that conductance suppression takes place when a dominant conduction channel exists ($\tau_1 > 0.5$). Furthermore, when the vibration activation is manifested as conductance suppression, the mode is found to have longitudinal symmetry, suggesting that the dominant channel is symmetric with respect to the junction axis.

Conductance enhancement was observed mainly below 0.7G₀. This observation is expected when all channels have transmission probabilities of $\tau < 0.5$. However, focusing on junctions with high conductance value, shot noise measurements reveal that vibration activation is manifested as conductance enhancement also in junctions with $\tau_1 > 0.5$, suggesting coupling of vibration modes to low transmitting channels (τ_2 or τ_3). Indeed, we find a different vibration mode, showing conductance enhancement and transverse symmetry. Applying the single-channel models in this case and assuming coupling of this vibration mode to a secondary channel lead to an unexpected large change in conductance with respect to the conductance contribution of the second channel. Alternatively, the appearance of conductance enhancement when $\tau_1 > 0.5$ can be explained outside the framework of the single-channel models by scattering between channels induced by vibration activation, according to symmetry considerations.

This work shows that although the single-channel models can explain a large variety of observations in multichannel junctions, the effect of vibration activation on conductance can involve scattering between channels. In order to have a more comprehensive understanding of electron–vibration interactions in a variety of atomic-scale junctions, the development of models that take into consideration more than a single conduction channel and account for possible interactions between channels is required.

EXPERIMENTAL METHODS

Formation of Molecular Junctions. Both Pt/benzene and Pt/CO₂ molecular junctions were constructed using a mechanically controllable break junction (MCBJ)³⁷ at 4.2 K. A small notch is cut in the middle of a Pt wire (99.99%, 0.1 mm diameter, Goodfellow), which is then glued to a flexible and isolated substrate. A three-point bending configuration in cryogenic vacuum conditions is used in order to break the wire at the notch to form an adjustable gap between two ultraclean tips. A piezoelectric element is used for fine bending of the substrate in order to control the distance between the electrodes with sub-angstrom resolution. Before dosing the sample with molecules, the formation of a clean Pt contact is verified by

conductance histograms. The target molecules, namely, benzene (99.97% purity, Sigma Aldrich) and CO₂ (99.995% purity, Gas Technologies), are introduced to the junction through a heated capillary while the sample is kept at cryogenic temperatures.³⁴ Before insertion, benzene was degassed by several freeze–pump–thaw cycles. CO₂ was inserted after the vacuum system was baked out, evacuated, and dosed, repeatedly. Benzene and CO₂ dosing was controlled by a needle-valve at the top of the capillary and by the capillary temperature. After the introduction of molecules, the formation of molecular junctions is indicated by a significant change in the conductance histogram and the detection of vibration modes by differential conductance measurements. For both Pt/benzene and

Pt/CO₂ junctions, the insertion of molecules was repeated for different samples and different dosing times, resulting in similar features in the conductance histograms, in very good agreement with previous results.³³

Differential Conductance Measurements. Differential conductance measurements (dI/dV) are performed using a Stanford Research SR830 lock-in amplifier. The lock-in produces an ac modulation signal of 1 mVrms at a frequency of 3.777 kHz, which is added to a dc signal.

After squeezing the junction to have $\sim 70G_0$, the electrodes are pulled apart until a new stable contact is formed with a conductance below the typical atomic conductance of Pt ($<1.5G_0$). At this point the interelectrode distance is fixed and a differential conductance curve is recorded while the dc voltage between the electrodes is swept. Only spectra showing a clear signature of conductance enhancement (i.e., as in Figure 1a) or suppression (Figure 1b) were considered in the analysis.

Shot Noise Measurements. Noise measurements and the determination of channel distribution are done as described in ref 44. Before and after each set of shot noise measurements a dI/dV spectrum is recorded to confirm that the contact maintains its stability during the noise measurement. Only measurements with deviation smaller than $0.04G_0$ in the zero-bias conductance between the two spectra are considered. dI/dV measurements and shot noise are measured using two switchable circuits. When combined with shot noise, dI/dV measurements are performed by a lock-in technique realized by a LabVIEW code. The noise, which is averaged over 5000 noise spectra, is measured as a function of frequency at different bias voltage applied to the junction. The transmission probabilities are obtained using the numerical approach, described in ref 44, under the assumption of $N = 6$ channels at the most. This assumption is easily tested by using $N + 1$ channels to obtain a similar solution.

Conflict of Interest: The authors declare no competing financial interest.

Acknowledgment. We thank A. Nitzan and K. Kaasbjerg for helpful discussions. O.T. thanks the Harold Perlman Family for their support and acknowledges funding by the Israel Science Foundation Grant No. 1313/10, the German-Israeli Foundation Grant No. I-2237-2048.14/2009, and the Minerva Foundation Grant No. 711136.

REFERENCES AND NOTES

1. Buttiker, M.; Imry, Y.; Landauer, R.; Pinhas, S. Generalized Many-Channel Conductance Formula with Application to Small Rings. *Phys. Rev. B* **1985**, *31*, 6207–6215.
2. Buttiker, M. Scattering-Theory of Current and Intensity Noise Correlations in Conductors and Wave Guides. *Phys. Rev. B* **1992**, *46*, 12485–12507.
3. Scheer, E.; Agrait, N.; Cuevas, J. C.; Yeyati, A. L.; Ludoph, B.; Martin-Rodero, A.; Bollinger, G. R.; van Ruitenbeek, J. M.; Urbina, C. The Signature of Chemical Valence in the Electrical Conduction Through a Single-Atom Contact. *Nature* **1998**, *394*, 154–157.
4. Cuevas, J. C.; Yeyati, A. L.; Martin-Rodero, A. Microscopic Origin of Conducting Channels in Metallic Atomic-Size Contacts. *Phys. Rev. Lett.* **1998**, *80*, 1066–1069.
5. Solomon, G. C.; Gagliardi, A.; Pecchia, A.; Frauenheim, T.; Di Carlo, A.; Reimers, J. R.; Hush, N. S. Molecular Origins of Conduction Channels Observed in Shot-Noise Measurements. *Nano Lett.* **2006**, *6*, 2431–2437.
6. Stipe, B. C.; Rezaei, M. A.; Ho, W. Single-Molecule Vibrational Spectroscopy and Microscopy. *Science* **1998**, *280*, 1732–1735.
7. Agrait, N.; Untiedt, C.; Rubio-Bollinger, G.; Vieira, S. Onset of Energy Dissipation in Ballistic Atomic Wires. *Phys. Rev. Lett.* **2002**, *88*, 216803.
8. Djukic, D.; Thygesen, K. S.; Untiedt, C.; Smit, R. H. M.; Jacobsen, K. W.; van Ruitenbeek, J. M. Stretching Dependence of the Vibration Modes of a Single-Molecule Pt-H₂-Pt bridge. *Phys. Rev. B* **2005**, *71*, 161402.
9. Hihath, J.; Arroyo, C. R.; Rubio-Bollinger, G.; Tao, N. J.; Agrait, N. Study of Electron-Phonon Interactions in a Single Molecule Covalently Connected to Two Electrodes. *Nano Lett.* **2008**, *8*, 1673–1678.
10. Paulsson, M.; Frederiksen, T.; Brandbyge, M. Modeling Inelastic Phonon Scattering in Atomic and Molecular Wire Junctions. *Phys. Rev. B* **2005**, *72*, 201101.
11. de la Vega, L.; Martin-Rodero, A.; Agrait, N.; Yeyati, A. L. Universal Features of Electron-Phonon Interactions in Atomic Wires. *Phys. Rev. B* **2006**, *73*, 075428.
12. Thijssen, W. H. A.; Strange, M.; de Brugh, J. M. J. A.; van Ruitenbeek, J. M. Formation and Properties of Metal-Oxygen Atomic Chains. *New J. Phys.* **2008**, *10*, 033005.
13. Kim, Y.; Pietsch, T.; Erbe, A.; Belzig, W.; Scheer, E. Benzenedithiol: A Broad-Range Single-Channel Molecular Conductor. *Nano Lett.* **2011**, *11*, 3734–3738.
14. Kumar, M.; Avriller, R.; Yeyati, A. L.; van Ruitenbeek, J. M. Detection of Vibration-Mode Scattering in Electronic Shot Noise. *Phys. Rev. Lett.* **2012**, *108*, 146602.
15. Matsushita, R.; Kaneko, S.; Nakazumi, T.; Kiguchi, M. Effect of Metal-Molecule Contact on Electron-Vibration Interaction in Single Hydrogen Molecule Junction. *Phys. Rev. B* **2011**, *84*, 245412.
16. Galperin, M.; Ratner, M. A.; Nitzan, A. Inelastic Electron Tunneling Spectroscopy in Molecular Junctions: Peaks and Dips. *J. Chem. Phys.* **2004**, *121*, 11965–11979.
17. Viljas, J. K.; Cuevas, J. C.; Pauly, F.; Hafner, M. Electron-Vibration Interaction in Transport Through Atomic Gold Wires. *Phys. Rev. B* **2005**, *72*, 245415.
18. Galperin, M.; Nitzan, A.; Ratner, M. A. Inelastic Tunneling Effects on Noise Properties of Molecular Junctions. *Phys. Rev. B* **2006**, *74*, 075326.
19. Frederiksen, T.; Lorente, N.; Paulsson, M.; Brandbyge, M. From Tunneling to Contact: Inelastic Signals in an Atomic Gold Junction from First Principles. *Phys. Rev. B* **2007**, *75*, 235441.
20. Egger, R.; Gogolin, A. O. Vibration-Induced Correction to the Current through a Single Molecule. *Phys. Rev. B* **2008**, *77*, 113405.
21. Monturet, S.; Lorente, N. Inelastic Effects in Electron Transport Studied with Wave Packet Propagation. *Phys. Rev. B* **2008**, *78*, 035445.
22. Entin-Wohlman, O.; Imry, Y.; Aharonov, A. Voltage-Induced Singularities in Transport through Molecular Junctions. *Phys. Rev. B* **2009**, *80*, 035417.
23. Avriller, R.; Yeyati, A. L. Electron-Phonon Interaction and Full Counting Statistics in Molecular Junctions. *Phys. Rev. B* **2009**, *80*, 041309.
24. Haupt, F.; Novotny, T.; Belzig, W. Phonon-Assisted Current Noise in Molecular Junctions. *Phys. Rev. Lett.* **2009**, *103*, 136601.
25. Schmidt, T. L.; Komnik, A. Charge Transfer Statistics of a Molecular Quantum Dot with a Vibrational Degree of Freedom. *Phys. Rev. B* **2009**, *80*, 041307.
26. Halbritter, A.; Makk, P.; Csonka, S.; Mihály, G. Huge Negative Differential Conductance in Au-H₂ Molecular Nanojunctions. *Phys. Rev. B* **2008**, *77*, 075402.
27. Jaklevic, R. C.; Lambe, J. Molecular Vibration Spectra by Electron Tunneling. *Phys. Rev. Lett.* **1966**, *17*, 1139–1140.
28. Lambe, J.; Jaklevic, R. C. Molecular Vibration Spectra by Inelastic Electron Tunneling. *Phys. Rev.* **1968**, *165*, 821–832.
29. Smit, R. H. M.; Noat, Y.; Untiedt, C.; Lang, N. D.; van Hemert, M. C.; van Ruitenbeek, J. M. Measurement of the Conductance of a Hydrogen Molecule. *Nature* **2002**, *419*, 906–909.
30. Pascual, J. I.; Jackiw, J. J.; Song, Z.; Weiss, P. S.; Conrad, H.; Rust, H. P. Adsorbate-Substrate Vibrational Modes of Benzene on Ag(110) Resolved with Scanning Tunneling Spectroscopy. *Phys. Rev. Lett.* **2001**, *86*, 1050–1053.
31. Yu, L. H.; Keane, Z. K.; Ciszek, J. W.; Cheng, L.; Stewart, M. P.; Tour, J. M.; Natelson, D. Inelastic Electron Tunneling via Molecular Vibrations in Single-Molecule Transistors. *Phys. Rev. Lett.* **2004**, *93*, 266802.
32. Liu, N.; Pradhan, N. A.; Ho, W. Vibronic States in Single Molecules: C₆₀ and C₇₀ on Ultrathin Al₂O₃ Films. *J. Chem. Phys.* **2004**, *120*, 11371–11375.

33. Kiguchi, M.; Tal, O.; Wohlthat, S.; Pauly, F.; Krieger, M.; Djukic, D.; Cuevas, J. C.; van Ruitenbeek, J. M. Highly Conductive Molecular Junctions Based on Direct Binding of Benzene to Platinum Electrodes. *Phys. Rev. Lett.* **2008**, *101*, 046801.
34. Tal, O.; Kiguchi, M.; Thijssen, W. H. A.; Djukic, D.; Untiedt, C.; Smit, R. H. M.; van Ruitenbeek, J. M. Molecular Signature of Highly Conductive Metal-Molecule-Metal Junctions. *Phys. Rev. B* **2009**, *80*, 085427.
35. Fock, J.; Sorensen, J. K.; Lortscher, E.; Vosch, T.; Martin, C. A.; Riel, H.; Kilsa, K.; Bjornholm, T.; van der Zant, H. A Statistical Approach to Inelastic Electron Tunneling Spectroscopy on Fullerene-Terminated Molecules. *Phys. Chem. Chem. Phys.* **2011**, *13*, 14325–14332.
36. Bruot, C.; Hihath, J.; Tao, N. J. Mechanically Controlled Molecular Orbital Alignment in Single Molecule Junctions. *Nat. Nanotechnol.* **2012**, *7*, 35–40.
37. Muller, C. J.; van Ruitenbeek, J. M.; de Jongh, L. J. Experimental-Observation of the Transition from Weak Link to Tunnel Junction. *Phys. C (Amsterdam, Neth.)* **1992**, *191*, 485–504.
38. Tal, O.; Krieger, M.; Leerink, B.; van Ruitenbeek, J. M. Electron-Vibration Interaction in Single-Molecule Junctions: From Contact to Tunneling Regimes. *Phys. Rev. Lett.* **2008**, *100*, 196804.
39. Yelin, T.; Vardimon, R.; Kuritz, N.; Korytar, R.; Bagrets, A.; Evers, F.; Kronik, L.; Tal, O. Atomically Wired Molecular Junctions: Connecting a Single Organic Molecule by Chains of Metal Atoms. *Nano Lett.* **2013**, *13*, 956–1961.
40. Paulsson, M.; Frederiksen, T.; Ueba, H.; Lorente, N.; Brandbyge, M. Unified Description of Inelastic Propensity Rules for Electron Transport through Nanoscale Junctions. *Phys. Rev. Lett.* **2008**, *100*, 226604.
41. Nakazumi, T.; Kaneko, S.; Matsushita, R.; Kiguchi, M. Electric Conductance of Single Ethylene and Acetylene Molecules Bridging between Pt Electrodes. *J. Phys. Chem. C* **2012**, *116*, 18250–18255.
42. Bergfield, J. P.; Barr, J. D.; Stafford, C. A. The Number of Transmission Channels through a Single-Molecule Junction. *ACS Nano* **2011**, *5*, 2707–2714.
43. Blanter, Y. M.; Buttiker, M. Shot Noise in Mesoscopic Conductors. *Phys. Rep.* **2000**, *336*, 1–166.
44. Vardimon, R.; Klionsky, M.; Tal, O. Experimental Determination of Conduction Channels in Atomic Scale Conductors Based on Shot Noise Measurements. *Phys. Rev. B* **2013**, *88*, 161404.
45. Bohler, T.; Edtbauer, A.; Scheer, E. Point-Contact Spectroscopy on Aluminium Atomic-Size Contacts: Longitudinal and Transverse Vibronic Excitations. *New J. Phys.* **2009**, *11*, 013036.
46. Troisi, A.; Ratner, M. A. Propensity Rules for Inelastic Electron Tunneling Spectroscopy of Single-Molecule Transport Junctions. *J. Chem. Phys.* **2006**, *125*, 214709.
47. Gagliardi, A.; Solomon, G. C.; Pecchia, A.; Frauenheim, T.; Di Carlo, A.; Hush, N. S.; Reimers, J. R. A Priori Method for Propensity Rules for Inelastic Electron Tunneling Spectroscopy of Single-Molecule Conduction. *Phys. Rev. B* **2007**, *75*, 174306.
48. Kristensen, I. S.; Paulsson, M.; Thygesen, K. S.; Jacobsen, K. W. Inelastic Scattering in Metal-H₂-Metal Junctions. *Phys. Rev. B* **2009**, *79*, 235411.